Environ. Sci. Technol. **2003**, *37,* 4804−4810

Treatment of Methyl *tert*-Butyl Ether Contaminated Water Using a Dense Medium Plasma Reactor: A Mechanistic and Kinetic Investigation

DEREK C. JOHNSON,[†]
VASGEN A. SHAMAMIAN,[‡]
JOHN H. CALLAHAN,[‡]
FERENCZ S. DENES,[§]
SORIN O. MANOLACHE,[§] AND
DAVID S. DANDY*,[†]

Department of Chemical Engineering, Colorado State University, Fort Collins, Colorado 80523, United States Naval Research Laboratory, Washington, D.C. 20375, and Center for Plasma Aided Manufacturing, Food Research Institute, University of Wisconsin—Madison, Madison, Wisconsin 53706

Plasma treatment of contaminated water appears to be a promising alternative for the oxidation of aqueous organic pollutants. This study examines the kinetic and oxidation mechanisms of methyl *tert*-butyl ether (MTBE) in a dense medium plasma (DMP) reactor utilizing gas chromatography−mass spectrometry and gas chromatography−thermal conductivity techniques. A rate law is developed for the removal of MTBE from an aqueous solution in the DMP reactor. Rate constants are also derived for three reactor configurations and two pin array spin rates. The oxidation products from the treatment of MTBE-contaminated water in the DMP reactor were found to be predominately carbon dioxide, with smaller amounts of acetone, *tert*-butyl formate, and formaldehyde. The lack of stable intermediate products suggests that the MTBE is, to some extent, oxidized directly to carbon dioxide, making the DMP reactor a promising tool in the future remediation of water. Chemical and physical mechanisms together with carbon balances are used to describe the formation of the oxidation products and the important aspects of the plasma discharge.

Introduction

Increasingly stringent regulations on wastewater discharge of organic compounds require that new, innovative technologies and methods of remediation be sought. Direct oxidation of organics using oxygen at normal/ambient conditions is too slow, and creating temperature and pressure conditions that increase the reaction rate such as those used in supercritical water oxidation are currently too costly (*1*). The oxidation of organic compounds to water and carbon dioxide is an appealing treatment method if complete oxidation can be achieved, or at the very least if the pollutant compounds can be converted into substances that do not require additional treatment. Thus, if the original compound is transformed into a more toxic material or a substance that is more difficult to remediate, the treatment process is deemed ineffective.

Ethers are volatile, explosive, odorous compounds used as solvents, refrigerants, artificial flavors, drugs, and softeners for plastics. An industrially significant ether and the focus of this study is methyl *tert*-butyl ether (MTBE). MTBE's principal use was as an anti-knock agent in gasoline, replacing tetraethyl lead, to ensure that catalytic converters used to reduce vehicle emissions are not deactivated by the deposition of lead from the exhaust (*2*, *3*). Ethers can be thought of as derivatives of water in which alkyl groups have replaced both hydrogen atoms. In fact, the C−O−C bond angle is only slightly larger than the H−O−H bond angle in water (*4*). Due to these similarities, ethers, especially short-chained ethers, are highly soluble and hence difficult to separate from water. Sufficient quantities of MTBE have been concentrated in groundwater through leaks in underground storage tanks and gasoline spills, causing nationwide concern. Advanced oxidation technologies (AOTs) are techniques that involve an input of energy—chemical, electrical, and/or radiative—into a fluid matrix to produce highly reactive oxidizing species, particularly hydroxyl radical, which in turn oxidize the organics, ideally to carbon dioxide and water. It is anticipated that AOTs will be able to chemically treat organic pollutants such as MTBE that have physical properties similar to the solvent, thereby alleviating the difficulties of treating this class of organic compounds present in water.

The most effective means of oxidizing organics and avoiding unwanted intermediate compounds is to use highly reactive species such as hydroxyl radical (•OH), singlet oxygen radical (•O), ozone (O_3), and hydrogen peroxide (H_2O_2) (*5*). The treatment of organically polluted water by radicals is extremely important not only in the purification of water but also for industrial processes as well. A number of processes, such as direct ozonation (*6*−*8*), ultraviolet radiation photolysis (*9*), high energy electron irradiation (*10*), supercritical water oxidation (*11*), wet air oxidation (*12*), UV−H_2O_2 oxidation (*13*), sonochemistry (*14*), photocatalysis (*15*), and several other AOTs, have been explored or are currently used to remove hazardous chemicals from contaminated water. Most of these methods focus on the in-situ production of hydroxyl radical. Commercial processes for the treatment of municipal wastewater and potable water have developed from research conducted on direct ozonation. Trace aqueous organic compounds have been degraded in the laboratory by processes, such as electrochemistry (*16*, *17*) and aqueous plasma (*18*−*22*), in which an electrical potential was applied across the fluid. Most of these processes have fallen short of their potential, whether due to energy inefficiency, low throughput, or an inability to scale up the process for industrial use. However, some AOTs such as plasma treatment are considered to be promising alternatives for the treatment of water pollutants.

Application of an aqueous plasma discharge to degrade organic pollutants in wastewater is a relatively new process. The process is characterized by the production of high oxidation potential species such as •OH, H_2O_2, and •O (*18*, *23*). Both corona and spark discharges can be created by a high-voltage discharge and are oxidation technologies in which energy is electrically introduced into an aqueous solution through a plasma channel. Under specific conditions, a strong electric field is produced which in turn produces a plasma discharge where many different reactive

* Corresponding author telephone: (970)491-7437; fax: (970)491-7369; e-mail: david.dandy@colostate.edu.
[†] Colorado State University.
[‡] United States Naval Research Laboratory.
[§] University of Wisconsin—Madison.

10.1021/es0263487 CCC: $25.00
Published on Web 09/10/2003

oxidizing species—•OH, •H, •O, •HO_2, •O_2^-, H_2O_2, O_3, and others—can subsist (*5*). These oxidizing species react with contaminant molecules. If complete oxidation is not achieved, it is desirable that pollutants are at least degraded into less hazardous hydrocarbons that are easier to remediate with a secondary treatment or disposed of completely.

The need for an energy-efficient method to treat organically polluted wastewater using highly oxidizing species has motivated research into the application of plasma generation by various types of electrical discharges, mainly corona/streamer discharges, spark/arc discharges, and glow discharge electrolysis. It is essential to develop an understanding of the chemical reaction mechanism and the chemical kinetics involved in these processes to be able to design, scale, and operate an electrical discharge reactor. It is also important to understand the mechanism and kinetics to assess the feasibility and efficiency of degrading organic compounds in plasma reactors.

Experimental Methods

Water contaminated with MTBE was treated using a new dense medium plasma (DMP) reactor developed by Denes and co-workers (*24*, *25*). The reactor was developed to react liquid/vapor-phase chemicals in an induced plasma state, using low-temperature plasma chemistry in which the liquid temperature remains relatively close to ambient temperatures. The advantages associated with this reactor are that (i) the reactions take place at atmospheric pressure and approximately room temperature, (ii) the discharge is controlled by electron flux, and (iii) large amounts of contaminated solution can be treated in either a batch or continuous mode in a scaled reactor. The DMP reactor can also emit a higher current, continuous discharge at lower voltages than previous point-to-plate aqueous plasma discharge reactors (*25*).

The DMP reactor in this study includes a reaction vessel containing a rotating upper electrode, a stationary lower electrode, cooling system, and gas introduction and discharge ports. The upper electrode is a pin array that can rotate at speeds up to 2500 rpm. Rotating the upper electrode distributes the sputtered metal from the pin electrodes evenly on the stationary electrode, preventing pitting and unwanted changes in the relative distance between the electrodes. Spinning the pin array also induces convective mass transfer, reducing mass transfer limitations that are apparent in high voltage point-to-plane plasma reactors. Rotating the upper electrode reduces the inception voltage by abating the effective distance between the pin electrodes and the stationary electrode.

Oxygen was injected into the system through the middle of the stationary electrode. A nebulizer was added to the original reactor configuration, allowing the liquid and oxygen to be transported coaxially through the middle of the stationary electrode to the reaction zone. This arrangement ensured that the solution in the reaction zone would be saturated with oxygen and that the oxygen bubble surface area would be maximized. This reactor configuration is referred to as the coaxial configuration, while an aqueous discharge without a nebulizer or coaxial flow is called the original configuration. The oxygen bubbles in the reaction zone reduce the apparent density of the medium between the stationary and pin electrodes, thereby lowering the inception voltage of the arcs as well as influencing the chemistry that is performed in and on the surface of the arc tubules. A third reactor configuration was developed to force the plasma discharge to occur only through oxygen; this third configuration prevented the aqueous solution from coming into contact with the plasma and is referred to as the gas discharge configuration. A schematic of the DMP reactor and its three reactor configurations can be found in the Supporting Information Figure S-1.

Gas transported through the system was vented through a valve at the top of the reaction vessel to keep the reactor at atmospheric pressure. A gas collection system was constructed with the capability to collect the gas samples and recirculate gas through the reaction zone (i.e., the plasma). Opaque Tedlar bags were used to collect and house the gas used in all DMP reactor experiments, preventing unwanted photolysis of the organics and loss to the walls.

The reactor was equipped with a cooling jacket to ensure the glass-to-metal seals in the reactor did not fail but, at the same time, allowing a controlled increase of the reaction medium temperature with time. Tap water, with a temperature of approximately 295 K, was flushed through the jacket at 1.17 ± 0.04 L/min. The initial temperature of the reaction media was 295 ± 1 K and reached steady state at 309 ± 1 K for all experiments.

The DMP reactor experiments were performed with an applied voltage of 200 ± 25 V and a resulting current of 1.00 ± 0.15 A. Because of the fluctuations in the plasma, neither the applied potential nor the current displayed steady-state behavior. Thus, the voltage and current readings represent time-averaged values while the error represents the fluctuation in each parameter. The pin array spin rate was 1000 rpm unless noted otherwise. Oxygen was bubbled through the middle of the stationary electrode at a flow rate of 400 mL/min and was not recirculated through the system. The electrode gap was 500 μm. A 250 mL, 50 ppm MTBE solution was recirculated through the middle of the stationary electrode coaxially with the oxygen at approximately 100 mL/min. In the first product study experiment, the contaminated solution was treated with plasma for 10 min. In the second product study experiment, the contaminated solution was treated with plasma for 11 min. All other operating conditions remained the same.

MTBE (≥99.8% purity) and the anticipated intermediate products of plasma treatment—*tert*-butyl formate (≥99.0% purity), acetone (≥99.8% purity), anhydrous *tert*-butyl alcohol (>99.5% purity), and formaldehyde (HPLC grade)—were obtained from Aldrich Chemical Co. Carbon dioxide calibrations were carried out by dilution of a Scott Gases standard. Millipore water was generated by a Milli-Q ultrapure water system and was used as the solvent.

The aqueous samples were analyzed using a Varian Saturn GC−MS system. The liquid samples collected from the DMP reactor, each 5.00 ± 0.02 mL, were diluted with 15.00 ± 0.04 mL of Millipore water in a Supelco 22-mL amber screw-top sampling vial. The samples were adsorbed onto a 100-μm poly(dimethylsiloxane) solid-phase microextraction (SPME) fiber. To adsorb the organics onto the fiber, a small stir bar was inserted into the sample vial. The vial was then placed in a 50 °C isothermal bath, and the stir bar was rotated at 300 rpm while the fiber was inserted into the vial through a septum for 13 min. The fiber was then immediately inserted into the injection port of the Varian GC. The samples were allowed to desorb in the GC injection port for approximately 10 min, conditioning the fiber for the subsequent sample. The injection port of the gas chromatographic instrument had a splitless flow into the column for 1 min to ensure that the desorbed species were trapped at the beginning of the column. After that, the gas flow rate became split with a 25:1 flow ratio for the remaining run time. The reactant and products were separated with a 30 m by 0.25 mm Phenomenex ZB-624 column, designed to separate volatile organic compounds. Two GC oven temperature control methods were used to analyze the compounds. The first method used an initial oven temperature of 0 °C, which was held at this temperature for 5 min, and then ramped at a rate of 10 °C/min to 100 °C. The oven temperature was then ramped at

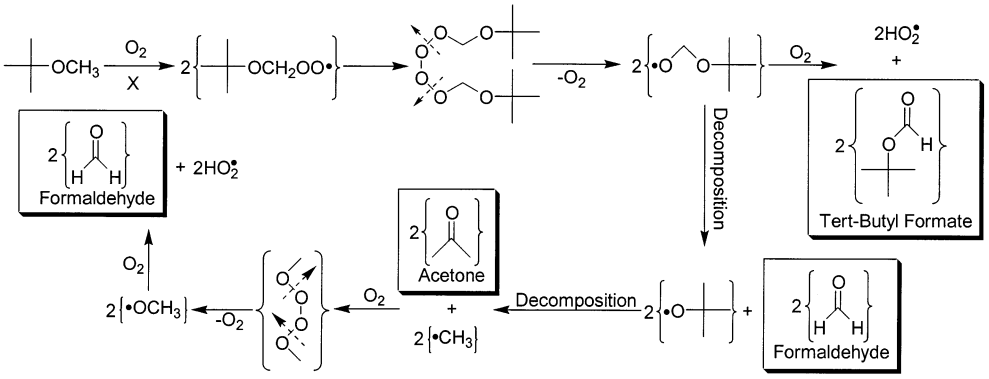

FIGURE 1. Reaction mechanism of the oxidation of MTBE in a DMP reactor by reactive oxidizing species (X) produced by the plasma discharge, site 1. The boxed compounds were identified in this study.

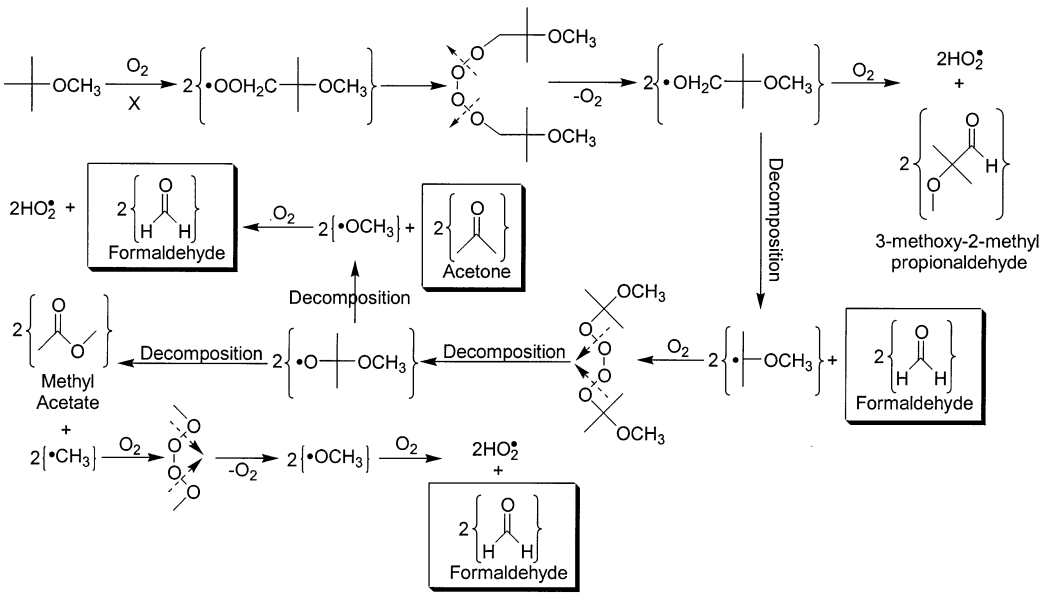

FIGURE 2. Reaction mechanism of the oxidation of MTBE in a DMP reactor by reactive oxidizing species (X) produced by the plasma discharge, site 2. The boxed compounds were identified in this study.

50 °C/min to a final temperature of 225 °C. Liquid nitrogen was used to cool the column below ambient temperatures. The second method had an initial oven temperature of 45 °C that was held for 1 min and then ramped at a rate of 10 °C/min to 120 °C. The oven temperature was ramped again at 30 °C/min to a final temperature of 200 °C. Ultrahigh-purity-grade helium was used as the carrier gas for both methods. The mass spectral analyses were performed in electron ionization mode with a scan range of 35−200 m/z and a background mass of 34 m/z.

Gas samples collected in Tedlar bags were analyzed using a Varian GC with a thermal conductivity detector (TCD). Carbon dioxide was separated in a 15 ft by $^1/_8$ in. 60/80 Carboxen 1000 packed column (Supelco). A 25-mL sample loop was purged using a pressurized analytical sample. After the loop was sufficiently purged, it was switched into the column flow, which was He at a rate of 30 mL/min. The column was maintained at 60 °C, and the thermal conductivity detector was at 220 °C.

Results

The principle products of the oxidation of MTBE by the DMP reactor are carbon dioxide (CO_2), acetone ($C(CH_3)_2O$), *tert*-butyl formate ($(CH_3)_3OCHO$), and formaldehyde (CH_2O). The mechanistic pathways used to predict the formation of oxidation products and to carry out the carbon balances are illustrated in Figures 1 and 2 (*26*).

Quantitative analysis of the total carbon in the DMP reactor at different times during treatment is presented in Figure 3. In this figure, the total amount of carbon (μmol) for the different species is plotted against treatment time. Real time sampling of carbon dioxide was not possible, so a cumulative CO_2 concentration was determined for each experiment. The total amount of carbon dioxide produced, in terms of carbon, is plotted for $t = 10$ and 11 min. Least-squares analysis was used to determine the error in the observed mass of reactant and products.

In the first experiment, 94.2 ± 5.8% of the carbon in the form of MTBE was accounted for after the 10-min reaction period. Of the total recovered carbon, 41.0 ± 2.6% was carbon dioxide, 33.8 ± 1.2% was gaseous MTBE (due to sparging of the aqueous organic), 12.4 ± 1.3% was formaldehyde, 4.46 ± 0.45% was acetone, 5.62 ± 0.23% was aqueous MTBE, and 2.75 ± 0.10% was *tert*-butyl formate. In the second experiment, 101.8 ± 5.7% of the carbon in the form of MTBE was accounted for after the 11-min reaction period. Of the total recovered carbon, 47.0 ± 2.9% was carbon dioxide, 33.9 ± 1.2% was gaseous MTBE (due to sparging of the aqueous organic), 10.0 ± 1.0% was formaldehyde, 3.45 ± 0.35% was acetone, 4.11 ± 0.17% was aqueous MTBE, and 1.55 ± 0.05% was *tert*-butyl formate. The reported errors represent a 96% confidence level.

The rate equation describing MTBE removal in the DMP reactor was found to be pseudo-first-order with respect to

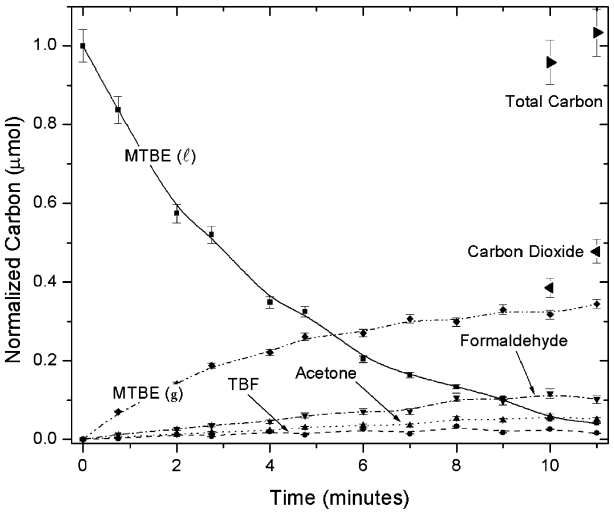

FIGURE 3. Carbon balance as a function of time for the oxidation of MTBE in a DMP reactor; 100% of the inputted carbon was recovered, within error, after the allotted treatment time of 10 and 11 min. The decrease of aqueous MTBE and the production of carbon dioxide, gaseous MTBE, *tert*-butyl formate, acetone, and formaldehyde are shown.

the MTBE concentration. The removal rate constants for MTBE in the gas-phase discharge configuration, coaxial configuration (1000 rpm), coaxial configuration (500 rpm), and original configuration were 0.47, 0.27, 0.22, and 0.18 s^{-1}, respectively.

Discussion

The experiments conducted on the DMP reactor focused on identifying the oxidation mechanism(s) of MTBE and the kinetics associated with the removal of this compound for three reactor configurations and two upper electrode spin rates. The DMP reactor utilizes plasma as the medium in which electric energy is transferred into a fluid media to degrade organic compounds. Plasma is a highly ionized gaseous phase consisting of electrons, ions, gas-phase atoms, molecules, and molecular fragments in various energy states. A plasma is generated by producing an electrical discharge in an insulating fluid such as water and may be classified as either a thermal (hot) or nonthermal (cold) plasma (*27*). A thermal plasma is comprised of gas atoms and electrons in local thermal equilibrium and is generally produced by high-pressure (atmospheric) spark/arc discharges (*27*). Thermal plasma channels also emit a broad spectrum of radiation, including ultraviolet (UV) radiation, and generate a powerful shock wave due to expansion against the surrounding fluid (*1*). The electrons produced from a thermal discharge have sufficient kinetic energy to completely dissociate any organic compound into its constituent atoms.

As discussed above, the plasma channel formed by a spark discharge is a high-temperature radiation source with a wide emission spectrum. The temperature of the plasma stream can exceed 10 000 K (*22*), which is sufficient to decompose virtually any organic compound. As atoms leave the plasma, they combine to form thermodynamically favored species; carbon from the organic molecule will react with oxygen initially present in the aqueous solution or in the bubbled gas to form carbon dioxide. On the basis of the observation that a significant amount of carbon dioxide was produced and there was a concomitant absence of stable intermediate dissociation products, it must be concluded that the bulk of the oxidation of MTBE occurs within the plasma channel of the DMP reactor. This result is advantageous in that MTBE is directly oxidized to carbon dioxide through a less complicated, faster chemical mechanism. However, the mass of MTBE that can be oxidized is directly proportional to the volume of the plasma produced in the reactor, making this route unfeasible in a single discharge reactor. However, the DMP reactor used in this study has 23 concurrent discharges, greatly increasing its potential to directly oxidize organic compounds within the plasma stream.

While direct oxidation within the plasma is an important degradation route, it has also been observed that MTBE undergoes oxidation within the liquid phase in the DMP reactor through reaction with reactive species. Hydroxyl radical and other unstable species form at the plasma−fluid interface (*28*). The plasma discharges are roughly cylindrical in shape and do not possess sufficient surface area to produce an appreciable amount of oxidizing radicals that can significantly reduce the concentration of an organic pollutant in a reasonable time. Diffusion and convective mass transfer can govern the rate with which an oxidizing radical produced on the surface of the arc and an organic molecule can interact outside the plasma stream. Since the radicals and the organics are constrained by the solvent molecules and remain trapped for approximately 10^{-11} s undergoing numerous collisions and the activation energy for radical−radical and radical−molecule reactions is low, the chemical reactions are facile (*29*). In a dilute organic solution, it is more probable for a radical to be trapped in the same solvent cage with another radical near the discharge site, initiating a quenching reaction. Thus, the quenching reaction rate is orders of magnitude higher than the rate of diffusion of an organic from the solution bulk to the reaction zone or of a radical from the reaction zone to the solution bulk. Therefore, it is unlikely that an appreciable amount of radical−organic solvent cage interactions will occur. Oxidation due to diffusion of organics to the radicals is possible; however, it would proceed slowly, and the efficiency would decrease as the organic concentration decreased. However, due to the numerous discharges produced in the DMP reactor, the plasma−fluid interfacial area is greatly increased. Spinning the pin array also increases the rate of mass transport in the DMP reactor as compared to single point-to-plane discharge reactors by inducing convective mass transfer.

To determine whether direct oxidation of MTBE to CO_2, without appreciable formation of stable intermediate products, occurred only when MTBE was cycled through the reaction zone, the reactor was modified to the gas discharge configuration. In this configuration, the plasma discharge traveled only through the oxygen introduced into the reactor through the middle of the stationary electrode. This mode of operation eliminated any possible MTBE electron impact dissociation reactions that may have been responsible for a significant portion of the degradation of MTBE and the subsequent formation of carbon dioxide. In this case, the MTBE oxidation process could only occur by reaction with active species. It was observed that, in this configuration, carbon dioxide was not produced and that the only oxidation products detected during the 10-min treatment experiment were the result of the primary and secondary oxidation pathways. Because of this, it is concluded that the oxidation of MTBE to carbon dioxide only occurs, on the time scale of these experiments, as a result of cycling the contaminated liquid through the reaction zone.

Reaction Mechanism. Reactive oxidizing species formed by the electrical discharge, particularly hydroxyl radical, are responsible for the initiation of the aqueous oxidation of MTBE in the coaxial and original DMP reactor configurations. While this oxidation pathway has been shown to be of secondary importance in the coaxial configuration, small quantities of stable products form that, depending on the precursor, could potentially be toxic. The importance of such products led to a more detailed study of this oxidation pathway. After the abstraction of a hydrogen atom from MTBE

by a reactive oxidizing species, it is oxidized by O_2 to form a peroxy radical. Two peroxy radicals may then combine but due to instabilities decompose into alkoxy radicals. Figures 1 and 2 provide details concerning the widely accepted oxidation mechanism of aqueous MTBE (*26*). It is the alkoxy radical that can undergo further decomposition, react with O_2, or isomerize. Isomerization in this system, however, is not likely due to the chemical structure of MTBE. Isomerization occurs predominantly by a 1−5 hydrogen abstraction mechanism, forming a six-member ring. However, MTBE only has the ability to form a five-member ring. The bond angle of the five-member ring invokes stress on the intermediate, making the rearrangement unlikely. Thus, isomerization is not considered. During decomposition, the carbon adjacent to the radical oxygen atom breaks its bond with the neighboring atom. When the alkoxy radical reacts with O_2, an aldehyde and a hydroperoxy radical ($HO_2^{\bullet}$) are formed.

The relative importance of the two mechanistic pathways—decomposition and reaction with O_2—for the MTBE alkoxy radical can be determined by examining the carbon product yields of the oxidation of MTBE. The alkoxy radical generated from the attack at site 1 reacts with O_2 to form *tert*-butyl formate or breaks the C−O bond to form formaldehyde and acetone, as illustrated in Figure 1. The alkoxy radical generated from the attack at site 2 reacts with O_2 to form 2-methoxy-2-methyl propionaldehyde (the latter of which was not observed in this study) or breaks the C−C bond to form formaldehyde, acetone, and methyl acetate (which was also not observed), as shown in Figure 2. The decomposition products, formaldehyde and acetone, are the most abundant oxidation products in the first product study experiment, with carbon yields of 12.4 ± 1.3% and 4.46 ± 0.45%, respectively. The principal decomposition products of the second product study experiment, formaldehyde and acetone, are also the most abundant oxidation products with carbon yields of 10.0 ± 1.0% and 3.45 ± 0.35%, respectively. *tert*-Butyl formate, formed via the O_2 reaction pathway, has relatively small carbon yields of 2.75 ± 0.10% and 1.55 ± 0.05% in the first and second product study experiments. As mentioned previously, thermal decomposition coupled with electron bombardment is clearly the dominant oxidation mechanism, with carbon dioxide accounting for 41.0 ± 2.6% and 47.0 ± 2.9% of the reacted carbon in the first and second product study experiments. Figure 3 shows the time evolution of the carbon balance for these experiments.

Removal Rate. The oxidation reaction rate of organics in an aqueous plasma reactor is dependent on many factors and proceeds by a complex set of chemical reactions, as discussed above. The reaction rate for the destruction of an organic molecule in an aqueous, point-to-plane discharge reactor has been observed to be a function of the current, applied voltage, salinity, electrode spacing, composition of the solution, pH, and the particular gas bubbled into the system (*30*). The removal rate of MTBE in the DMP reactor is also assumed to be dependent on these parameters. However, since the plasma characteristics are a function of the above parameters and the removal rate is dependent on the plasma as well as interphase mass transfer, a general rate equation, which depends on MTBE and active oxidizing species' concentrations and the flux of MTBE from the liquid to the gas phase, is

$$-\frac{dC_{MTBE}}{dt} = kC_{MTBE}{}^{m}C_A{}^{a}C_B{}^{b} \ldots C_N{}^{n} + \frac{A_I}{V_O}W_{MTBE} \quad (1)$$

where k is the reaction rate constant; C denotes species concentration; A, B, ..., N are active oxidizing species produced by the plasma discharge; A_I is the interfacial area; V_O is the volume of the oxygen; and W_{MTBE} is the flux of MTBE. However, even though the voltage and current

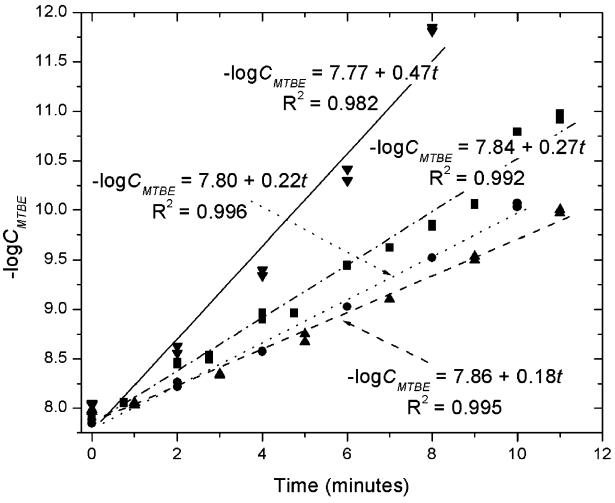

FIGURE 4. Plot of the −log(C_{MTBE}) vs time for the pseudo-first-order rate equation of the oxidation of MTBE in the coaxial configuration with a pin array spin rate of 1000 (■) and 500 rpm (●), the original configuration (▲), and the gas discharge configuration (▼).

fluctuate during the experiments, the applied power is constant, and as a result the rate of the plasma discharge is approximately constant. Therefore, the concentrations of the active oxidizing species are constant and can be combined with the reaction rate constant to produce an observed reaction rate constant, k_{rxn}. The flux of MTBE can be expressed as

$$W_{MTBE} = -C_{MTBE}D_{MTBE,H_2O}\nabla y_{MTBE} + y_{MTBE}(W_{MTBE} + W_{H_2O}), \quad (2)$$

where D_{MTBE,H_2O} is the diffusivity of MTBE in H_2O and y_{MTBE} is the mole fraction of MTBE. The first term in eq 2 represents the flux due to molecular diffusion produced by a concentration gradient, and the second term is the flux due to bulk fluid flow. However, when the solute is dilute in the solvent and there is no net flux of solvent, the flux due to bulk fluid motion is negligible when compared to the flux due to molecular diffusion. Thus, after simplifying and substituting for W_{MTBE} in eq 1 and including k_{rxn}, the rate equation simplifies to

$$-\frac{dC_{MTBE}}{dt} = C_{MTBE}\left(k_{rxn}C_{MTBE}^{m-1} + \frac{A_I}{V_O}D_{MTBE,H_2O}\nabla y_{MTBE}\right) \quad (3)$$

Since the reaction order (m) is not known, the equation cannot be integrated unless one is assumed and then compared to the data. If m is assumed to be 1 and the differential equation is integrated, the result is

$$\log C_{MTBE} = \log C_{MTBE_0} - k_{obs}t \quad (4)$$

where $k_{obs} = k_{rxn} + A_I D_{MTBE,H_2O}\nabla y_{MTBE}/V_O$. The plot of − log($C_{MTBE}$) versus t for the two product study experiments is linear, as shown in Figure 4. The agreement between eq 4 and the data indicates that the rate equation is pseudo-first-order with respect to the MTBE concentration. Furthermore, the reaction rate constant (k) is directly proportional to k_{obs}. Data for the removal of MTBE in two additional reactor configurations and an additional spin rate are also plotted in Figure 4. Since only one variable has been varied in each of these experiments, the effect of reactor configuration and pin array spin rate can be compared. Thus, the relative dependence of the reaction rate constant on salinity, electrode spacing, composition of the solution, pH, and gas

TABLE 1. Efficiency (*G*) of the DMP Reactor in Three Reactor Configurations for Removal of MTBE as a Function of Time[a]

gas discharge configuration			coaxial configuration (500 rpm)		
time (min)	x_t (%)	$G \times 10^9$ (mol/J)	time (min)	x_t (%)	$G \times 10^9$ (mol/J)
2	43.5	1.90	2	29.9	1.31
4	70.1	1.53	4	48.8	1.07
6	83.8	1.22	6	66.8	0.974
8	94.2	1.03	8	79.3	0.867
10	100	0.875	10	87.5	0.766
coaxial configuration (1000 rpm)			**original configuration**		
time (min)	x_t (%)	$G \times 10^9$ (mol/J)	time (min)	x_t (%)	$G \times 10^9$ (mol/J)
0.75	14.5	1.69	1	6.57	0.57
2	41.5	1.82	3	30.6	0.89
2.75	45.8	1.46	5	52.1	0.91
4	63.7	1.39	7	67.6	0.85
4.75	65.6	1.21	9	78.6	0.76
6	78.3	1.14	11	86.6	0.69
7	82.2	1.03			
8	85.4	0.934			
9	88.4	0.859			
10	94.2	0.824			
11	95.2	0.757			

[a] $V_s = 250$ mL, $P = 200$ W, and $C_o = 4.2 \times 10^{-4}$ M.

bubbled into the system could be determined at the same energy conditions with additional experimental data.

While the rate constant for the gas discharge configuration is more than double that of both the coaxial configuration at 500 rpm and the original configuration, none of the original MTBE is converted to carbon dioxide in the gas discharge configuration. The coaxial reactor configuration has a rate constant higher than that seen for the original configuration for a pin array spin rate of 1000 rpm. This is due to the additional flux of liquid through the reaction zone. However, due to the relatively small amount of carbon introduced into the reactor, the nebulizer did not have a significant net effect on the removal of MTBE from the solution, as shown in Figure 5. A small increase (approximately 2%, and outside the measurement errors) was seen after the 11-min treatment time. The greatest difference in the percent of aqueous MTBE removed from the fluid was at the initial and intermediate stages of the experiments. However, if a significantly contaminated aqueous solution was treated with the DMP reactor, the coaxial configuration would reduce the required treatment time due to the increase in oxidation efficiency seen at the beginning and intermediate stages of the MTBE experiments.

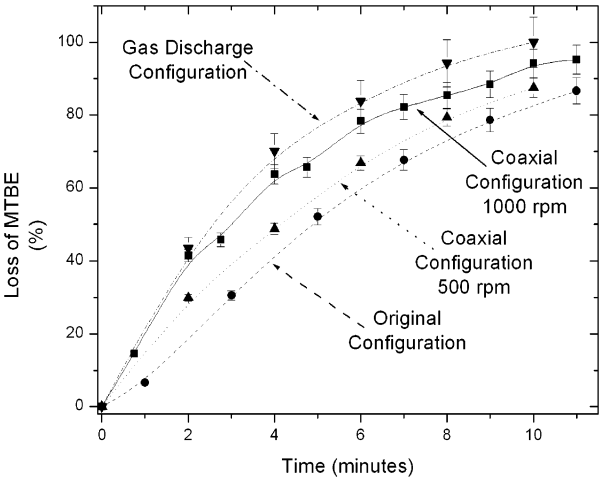

FIGURE 5. Plot of the percent loss of MTBE vs time in the DMP reactor comparing the performance of the coaxial configuration with a pin array spin rate of 1000 (■) and 500 rpm (▲), the original configuration (●), and the gas discharge configuration (▼).

Removal Efficiency. Given the power input, the volume of solution, and the removal of MTBE at a given time, the MTBE removal efficiency of the DMP reactor can be calculated for the various reactor configurations and spin rates. The removal efficiency (*G*) denotes the number of molecules removed or degraded with respect to a given amount of energy. The removal efficiency, which includes both chemical and physical attenuation mechanisms, is defined as

$$G_{x_t} = \frac{x_t C_o V_s}{tP} \tag{5}$$

where x_t is the fraction of MTBE removed or degraded at time t; C_o is the initial MTBE concentration; V_s is the volume of the aqueous solution; t is the time; and P is the input power. The removal efficiencies as a function of treatment time in the DMP reactor are shown in Table 1 for three reactor configurations and two pin array spin rates. The removal efficiency of the DMP reactor is also compared to results published in the literature in Table 2 using the G_{50} parameter. This value is calculated using eq 5 with $x_t = 0.5$ and using the time required to degrade or remove 50% of the original target molecule.

These experiments have yielded a number of important insights into the mechanistic pathways and kinetics for the oxidation of organic compounds in the DMP reactor. Most aqueous plasma reactors oxidize organics via attack by reactive oxidizing species produced by the plasma discharge;

TABLE 2. Comparison of the Efficiency of the DMP Reactor in Three Reactor Configurations to Other Plasma Discharge Technologies Found in the Literature Using the G_{50} Parameter

discharge description		$C_o \times 10^3$ (M)	V_s (L)	P (W)	E (mJ)	f (Hz)	t_{50} (min)	$G_{50} \times 10^9$ (mol/J)	ref
DMP reactor	coaxial (10^3 rpm)	0.42	0.25	200	na	na	3.0	1.46	this work
	coaxial (500 rpm)	0.42	0.25	200	na	na	4.3	1.02	
	original (10^3 rpm)	0.42	0.25	200	na	na	4.9	0.893	
	O_2 gas (10^3 rpm)	0.42	0.25	200	na	na	2.9	1.51	
corona	O_2 gas (MB)	0.019	0.10	0.20	na	na	60	1.32	*30*
	O_2 gas (MG)	0.016	0.10	0.20	na	na	60	1.11	
corona	air atmosphere	0.01	0.10	na	25	100	6	0.556	*31*
corona	air atmosphere	1.0	0.10	na	5.8	100	75	18.0	*32*
	Ar atmosphere	1.0	0.10	na	10.6	100	90	17.5	
corona	water	0.03	.55	na	1750	60	180	0.00728	*20*, *34*
corona	water	0.53	1.0	na	800	50	260	0.425	*1*, *34*
corona	water	0.53	0.25	na	880	48	7	3.74	*5*, *34*
corona	water	0.02	0.50	na	30	50	180	0.309	*33*, *34*

however, the DMP reactor has the ability to directly oxidize organic compounds directly to CO_2. The attenuation of MTBE in the DMP reactor also occurs by reaction with active species, as in most aqueous plasma discharge reactors, as well as interphase mass transfer. Another important feature of the DMP reactor is that the removal kinetics can be modeled as pseudo-first-order with respect to the original pollutant concentration. This is due to the fact that the oxidation of MTBE occurs within the volume of the arc, which remains relatively constant throughout the operating time of the reactor, the reactive species' concentrations remain relatively constant, and interphase mass transfer is a first-order rate process. It is also observed that the removal efficiency of the DMP reactor increases with an increase in spin rate and is a function of the reactor configuration, as shown in Figures 4 and 5. With further design improvements and reactor optimization, the DMP reactor may become a competitive wastewater treatment technology.

Acknowledgments

The authors acknowledge support for this work from the Office of Naval Research Grant N00014-00-WX2-1163 and the National Science Foundation's Fast Track to Work Scholarship Program. The authors also thank Dr. James E. Bulter, head of the Gas and Surface Dynamics Section at the Naval Research Laboratory, for his support.

Supporting Information Available

A schematic of the DMP reactor and its three reactor configurations. This material is available free of charge via the Internet at http://pubs.acs.org.

Literature Cited

(1) Sunka, P.; Babicky, V.; Clupek, M.; Lukes, P.; Simek, M.; Schmidt, J.; Cernak, M. *Plasma Sources Sci. Technol.* **1999**, *8*, 258−265.
(2) Riddick, J. A.; Bunger, W. B.; Sakano, T. K. *Organic Solvents, Physical Properties and Methods of Purification*, 4th ed.; Wiley: New York, 1986; pp 920−924.
(3) Sterner, O. *Chemistry, Health and Environment*; Wiley-VCH: New York, 1999; pp 21−22.
(4) Solomons, T. W. G. *Organic Chemistry*, 6th ed.; John Wiley & Sons: New York, 1996.
(5) Sun, B.; Sato, M.; Clements, J. S. *J. Phys. D*: *Appl. Phys.* **1999**, *32*, 1908−1915.
(6) Gurol, M. D.; Vatistas, R. *Water Res.* **1987**, *21*, 895−900.
(7) Hoigne, J.; Bader, H. *Water Res.* **1976**, *10*, 377−386.
(8) Hoigne, J.; Bader, H. *Ozone*: *Sci. Eng.* **1979**, *1*, 73−85.
(9) Glaze, W. H.; Kang, J. W.; Chapin, D. H. *Ozone*: *Sci. Eng.* **1987**, *9*, 335−352.
(10) Nickelsen, M. G.; Cooper, W. J.; Kurucz, C. N.; Waite, T. D. *Environ. Sci. Technol.* **1992**, *26*, 144−152.
(11) Thornton, T. D.; Savage, P. E. *J. Supercrit. Fluids* **1990**, *3*, 240−248.
(12) Joglekar, H. S.; Samant, S. D.; Joshi, J. B. *Water Res.* **1991**, *25*, 135−145.
(13) Legrini, O.; Oliveros, E.; Braun, A. M. *Chem. Rev.* **1993**, *93*, 671−698.
(14) Petrier, C.; Jiang, Y.; Lamy, M. F. *Environ. Sci. Technol.* **1998**, *32*, 1316−1318.
(15) Davis, A. P.; Huang, C. P. *Water Res.* **1990**, *24*, 543−550.
(16) DeSucre, V. S.; Watkinson, A. P. *Can. J. Chem. Eng.* **1981**, *59*, 52−59.
(17) Stucki, S.; Kotz, R.; Carcer, B.; Suter, W. *J. Appl. Electrochem.* **1991**, *21*, 99−104.
(18) Sun, B.; Sato, M.; Clements, J. S. *J. Electrost.* **1997**, *39*, 189−202.
(19) Sato, M.; Ohgiyama, T.; Clements, J. S. *IEEE Trans. Ind. Appl.* **1996**, *32*, 106−112.
(20) Joshi, A. A.; Locke, B. R.; Arce, P.; Finney, W. C. *J. Hazard. Mater.* **1995**, *41*, 3−30.
(21) Robinson, J. W.; Ham, M.; Balaster, A. N. *J. Appl. Phys.* **1973**, *44*, 72−75.
(22) Sun, B.; Sato, M.; Harano, A.; Clements, J. S. *J. Electrost.* **1998**, *43*, 115−126.
(23) Willberg, D. M.; Lang, P. S.; Hochemer, R. H.; Kratel, A.; Hoffmann, M. R. *Environ. Sci. Technol.* **1996**, *30*, 2526−2534.
(24) Denes, F. S.; Young, R. A. Apparatus for Reactions in Dense-Medium Plasmas. U.S. Patent 5,534,232, 1996.
(25) Manolache, S.; Somers, E. B.; Wong, A. C. L.; Shamamian, V.; Denes, F. *Environ. Sci. Technol.* **2001**, *35*, 3780−3785.
(26) Vollhardt, K. P. C.; Schore, N. E. *Organic Chemistry*, 2nd ed.; W. H. Freeman and Company: New York, 1994; pp 889−890.
(27) Lieberman, M. A.; Lichtenberg, A. J. *Principles of Plasma Discharges and Materials Processing*; John Wiley & Sons: New York, 1994.
(28) Roth, J. R. *Industrial Plasma Engineering*: *Vol. 1*, *Principles*; IOP Publishing Ltd: Philadelphia, 1995.
(29) Steinfeld, J. I.; Francisco, J. S.; Hase, W. L. *Chemical Kinetics and Dynamics*, 2nd ed.; Prentice Hall: Upper Saddle River, NY, 1999.
(30) Goheen, S. C.; Durhlam, D. E.; McCulloh, M.; Heath, W. O. *Proceedings of the Second International Symposium on Chemical Oxidation*, Nashville, TN, 1992.
(31) Hayashi, D.; Hoeben, W. F. L. M.; Dooms, G.; van Veldhuizen, E. M.; Ruthers, W. R.; Kroesen, G. M. W. *J. Phys. D*: *Appl. Phys.* **2000**, *33*, 1484−1486.
(32) Hoeben, W. F. L. M.; van Veldhuizen, E. M.; Rutgers, W. R.; Cramers, C. A. M. G.; Kroesen, G. M. W. *Plasma Sour. Sci. Technol.* **2000**, *9*, 361−369.
(33) van Veldhuizen, E. M.; Rutgers, W. R. *12th International Symposium on Plasma Chemistry*, Minneapolis, MN, 1995.
(34) Hoeben, W. F. L. M.; van Veldhuizen, E. M.; Rutgers, W. R.; Kroesen, G. M. W. *J. Phys. D*: *Appl. Phys.* **1999**, *32*, L133−L137.

Received for review November 20, 2002. Revised manuscript received July 16, 2003. Accepted July 30, 2003.

ES0263487